

Proceedings Article

# Modular MPI Component Test System

Eric Aderhold <sup>a,\*</sup> · Hannes Wieprecht <sup>b</sup> · Matthias Graeser <sup>a,b</sup>

<sup>a</sup>Fraunhofer Research Institution for Individualized and Cell-Based Medical Engineering IMTE, Lübeck, Germany

<sup>b</sup>Institute of Medical Engineering, University of Lübeck, Lübeck, Germany

\*Corresponding author, email: [eric.aderhold@imte.fraunhofer.de](mailto:eric.aderhold@imte.fraunhofer.de)

© 2023 Aderhold *et al.*; licensee Infinite Science Publishing GmbH

This is an Open Access article distributed under the terms of the Creative Commons Attribution License (<http://creativecommons.org/licenses/by/4.0>), which permits unrestricted use, distribution, and reproduction in any medium, provided the original work is properly cited.

## Abstract

The image quality of magnetic particle imaging depends on the interference-free measurement of the particle spectrum. Systematic errors due to harmonic distortions in the components used for implementation complicate the development of efficient imaging devices. To test the suitability of parts for the development of MPI scanners, a test system was developed in which the components to be tested can be integrated, to evaluate their suitability using the measured spectrum. Different forms of connectors integrated into the high-current path were analyzed for their influence on the signal quality using this test system. An evaluation of these components can be made from the clearly visible distortions in the spectrum recorded with the high-sensitive test system.

## I. Introduction

Magnetic particle imaging (MPI) promises to achieve a high spatial and temporal resolution as well as a high sensitivity [1]. It is based on the nonlinear magnetization behavior of magnetic nanoparticles (MNP) and relies on external oscillating magnetic fields generating a unique particle response. This response, which consists of the higher harmonics of the excitation frequency, is recorded with receive coils and provides the frequency spectra used to reconstruct the images.

Systematic errors, where harmonic distortions occur due to the implementation, overlaying the actual particle signal are problematic. Those errors can occur, e.g., due to the usage of ferromagnetic materials in parts or assemblies used to build the scanner or by nonlinear characteristics of the electrical components. As those nonlinearities cause signals on the exact same frequencies as the MNPs, image artifacts arise.

Considering MPI scanners as an industrial product and at the same time aiming for high modularization and easy maintainability, purchased parts become inevitable in the implementation. Those are usually cheaper and more efficient than in-house production and benefit

from the specialization of the corresponding suppliers. The major disadvantage is, that due to the complexity of the products and manufacturing technologies, their suitability for MPI devices is not always clearly evident. The use of unsuitable purchased parts in a scanner can lead to costly and time-consuming debugging. One option to determine the suitability of (purchased) components is to test them on a component test system. The following paper presents a sensitive modular component test system.

## II. Methods and materials

As test system a 1D magnet particle spectrometer (MPS), without offset fields, is built in a typical approach for the transmit and receive chain, consisting of an I/O device, a power amplifier, a transmit filter, an impedance matching and transmit coil, as well as a receive coil, a receive filter and a low noise amplifier (LNA). In order to perform the test under conditions comparable to those in parallel developed MPI scanners, the high current circuit was built to generate a magnetic field of 25 mT in the transmit coil with a current of about 34 A at a frequency

of  $f_0 = 25$  kHz. The developed coil holder with a height of 45.5 mm and a diameter of 20 mm was printed with a high-temperature material in order to guarantee dimensional stability even with longer running times and greater temperature development of the transmit coil. The send coil was realized with two layers of 15 inner and 14 outer windings made of litz wire with 2000 strands of 0.05 mm diameter. The coil-specific parameters were measured as  $L = 9.63 \mu\text{H}$  and  $R_{\text{DC}} \approx 17 \text{ m}\Omega$ .

To enable maximum active power transmission, an LCC matching network as impedance matching to the  $8 \Omega$  nominal impedance of the power amplifier was designed and tuned [2]. For the receive path two coils were implemented. The primary receive coil was designed as a first order gradiometric coil with six turns each as the receive and counter-wound compensating part, whose distance symmetrically around the central plane is 15 mm. The designed core body was additively manufactured and wound with litz wire (515 x 0.02 mm). In addition, another winding was implemented in the central plane as a reference coil. A voltage of 0.45 V is induced in this single winding at 25 mT, thus enabling a reference measurement of the transmitted field. Alternatively, the two available receive paths can be interchanged so that the reference coil serves as the receive coil and the attenuation of  $-70.8$  dB by the gradiometer is not applied. In this way, distortions from the transmit chain, which are generated by the test objects but attenuated to the noise level by the gradiometer, can be recorded and evaluated.

Within this setup, various components can be inserted at any point in the high-current circuit to test their influence on signal quality. In order to allow easy replacement while minimizing overall changes in the system so that only individual parts can be properly analyzed, all components are housed in individual aluminum enclosures (Figure 1). Therefore, any component or assembly can be easily replaced or customized by unscrewing and unsoldering. One compartment accommodates by default only one cable path to allow the insertion of additional elements, e.g. connectors.

The evaluation is performed on the recorded spectrum, after data acquisition (based on [3]), data limiting, phase and background correction and Fourier transformation of the time signals. In accordance with the initial modeled measurement protocol, a test cycle comprises the recording of two background measurements and a signal or component measurement, so that the comparison of the respective background-corrected empty and component measurements is possible.

As an indicator for the usability of a device under test (DUT), in addition to the visual comparison of the spectrum, the following indicator, as sum of the relative errors of the harmonics, is proposed:

$$\eta_{\text{DUT}} = \sum_{k=2}^N \frac{|\hat{a}_{k_{\text{DUT}}} - \hat{a}_{k_0}|}{\hat{a}_{k_0}},$$

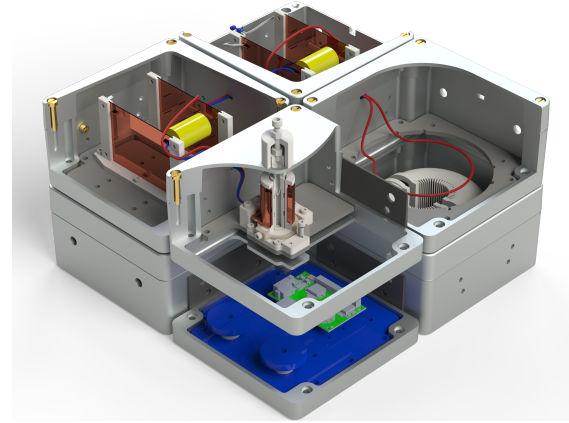


**Figure 1:** Construction overview of the test system including the transmit and receive coils, the high-current circuit and the receive filter arranged underneath.

where  $\hat{a}_{k_0}$  is the amplitude of the  $k$ -th harmonic of the initial empty measurement  $\hat{a}_{k_{\text{DUT}}}$  the respective amplitude of the device under test, and  $N$  the number of harmonics to be considered. Due to the bandwidth limitation of the used low-noise amplifier to 1 MHz, only harmonic components up to this frequency are used in this evaluation.

First component tests were done with the following test objects [4, 5]:

- M2 LEMO® 2B series connector
- M5 Reely XT-60 connector
- M6 Cable shoes connected by brass screw
- M7 Cable shoes connected by magnetic stainless steel screw

### III. Results

The development and implementation resulted in a functional one-dimensional spectrometer, with stable background, capable of measuring particle samples and enabling component testing.

In order to test the time stability of the spectrometer, twenty not background corrected measurements were made on two days each about one hour apart and the average of the harmonic distortion of the empty measurements was determined ( $\mu = 0.041\%$ ;  $\sigma = 0.001\%$ ). In addition, the temperature dependence of the system was considered, and a heating of  $9.5$  °C inside the send coil was found for a continuous measurement of 120 s with a 25 mT drive field, while the differences of the background spectra was found insignificant.

For comparability with existing spectrometers, a particle sample containing 10  $\mu\text{l}$  of undiluted nanoparticles (perimag®, plain) was measured using the gradiometric receive coil. The corresponding spectrum can be found in Figure 2, where the stable noise floor of below  $2 \times 10^{-5}$  V for frequencies above 100 kHz can be seen.

$\eta_{M1}$	$\eta_{M2}$	$\eta_{M5}$	$\eta_{M6}$	$\eta_{M7}$
0.0	131.6	48.8	27.7	332.8
0.0	585.1	863.2	36.8	18178

**Table 1:** Calculated suitability indicators  $\eta_{MX}$  for the first performed device tests using the gradiometric (first row) and non gradiometric (second row) receive path.

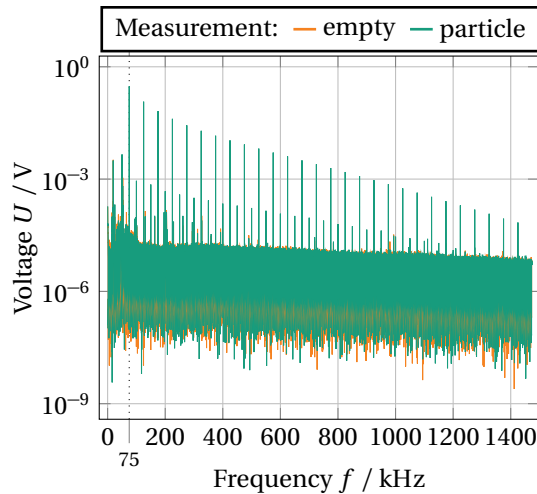


**Figure 2:** Background corrected particle and empty measurement of the gradiometric receive path in the test bench.

First component tests were performed for different connector types within the high current circuit, including two commercially available plug connectors. The influence of the tested parts on the spectrum is exemplary shown for the amplitudes of the first eight harmonics in Figure 3, since for higher frequencies the deviation does not rise above the background level, while using the gradiometric receive coil.

If the same tests are performed with the alternative receive path, which contains a single coil and therefore attenuates the disturbances from the transmit path significantly less, a similar evaluation sequence can be made for the tested components regardless to significantly increased amplitudes. In this second measurement cycle, the measurement *M6* shows comparable amplitude ratios as in the previous gradiometric measurements. For measurements *M5* and *M7*, the amplitudes can be clearly distinguished from the background up to the 19th harmonic, and for *M2* up to the 11th. The corresponding indicator values for both types of measurement are listed in Table 1.

## IV. Conclusion and Discussion

A modular component test system was developed using the principle concept of an MPS. First tests of connectors were carried out showing varying impacts on the signal quality.

In addition to a visual evaluation of the spectrum, initial attempts were made to introduce an indicator for

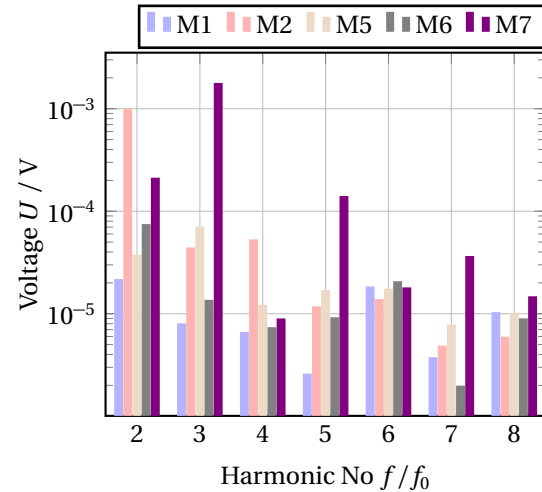


**Figure 3:** Amplitude of the first harmonics from background corrected measurements of different connectors. *M1* showing the amplitude for the empty reference measurement.

the suitability of the device under test in MPI scanner implementation. In order to obtain comparable results, dedicated test protocols should be developed, to ensure that the observed harmonic distortions can be fully assigned to the test object. Also, a test series should be set up to analyze the influence of the test object on an actual to be measured particle spectrum. This test would allow not only the measurement of the pure distortion of the signals by the device under test, but also show to what degree they would disturb actual particle measurements.

Field strength and phase control can improve the stability of the measurement system. On the software side, the transfer functions will be recorded and integrated, in order to separate the recorded signals from the basic hardware state and to place the results on a comparable basis (magnetic moment of the particles, cf. [6]). Using the test protocol, spectrum and indicator value a possibly, test part dependent, decision support could be developed to obtain a fast assessment of the components. However, since such a decision aid must include a risk assessment as well as the error potential arising from the use of the test object in an MPI scanner, this requires further analyses and considerations.

## Acknowledgments

Research funding: The Fraunhofer IMTE is supported by the EU (EFRE) and the State Schleswig-Holstein, Germany (Project: IMTE – Grant: 124 20002/LPW-E1.1.1/1536).

## Author's statement

Authors state no conflict of interest.

## References

- [1] A. Neumann et. al. Recent developments in magnetic particle imaging. *Journal of Magnetism and Magnetic Materials*, 550:169037, 2022, doi:[10.1016/j.jmmm.2022.169037](https://doi.org/10.1016/j.jmmm.2022.169037).
- [2] A. Behrends et. al. A standard procedure for implementation and automatic correction of lcc matching networks. *International Journal on Magnetic Particle Imaging*, pp. Vol 6 No 2 Suppl. 1 (2020), 2020, doi:[10.18416/IJMPI.2020.2009036](https://doi.org/10.18416/IJMPI.2020.2009036).
- [3] N Hackelberg et. al. A flexible high-performance signal generation and digitization platform based on low-cost hardware. *International Journal on Magnetic Particle Imaging*, pp. Vol 8 No 1 Suppl 1 (2022), 2022, doi:[10.18416/IJMPI.2022.2203063](https://doi.org/10.18416/IJMPI.2022.2203063).
- [4] S. LEMO S.A. (). Datasheet lemo 2b.302 series. note = accessed on 13.01.2023", URL: <https://www.lemo.com/pdf/EGG.2B.302.CLL.pdf%20and%20https://www.lemo.com/pdf/FGG.2B.302.CLAD82.pdf>.
- [5] G. Conrad Electronic SE. (). Datasheet xt60-f and xt60-m. accessed on 13.01.2023, URL: <https://asset.conrad.com/media10/add/160267/c1/-/en/002206316DS00/datenblatt-2195505-reely-re-6586515-akku-stecker-xt60-35-mm-zum-loeten-1-st.pdf>.
- [6] F Thieben et. al. On the receive path calibration of magnetic particle imaging systems. *IEEE Transactions on Instrumentation and Measurement*, pp. 1–1, 2022, doi:[10.1109/tim.2022.3219461](https://doi.org/10.1109/tim.2022.3219461).